New Journal of Physics
The open access journal for physics

Coherent two-dimensional electronic spectroscopy in the Soret band of a chiral porphyrin dimer

Federico Koch[1], Martin Kullmann[1], Ulrike Selig[1], Patrick Nuernberger[1], Daniel C G Götz[2,3], Gerhard Bringmann[2] and Tobias Brixner[1,4]

[1] Institut für Physikalische und Theoretische Chemie, Universität Würzburg, Am Hubland, D-97074 Würzburg, Germany
[2] Institut für Organische Chemie, Universität Würzburg, Am Hubland, D-97074 Würzburg, Germany
E-mail: brixner@phys-chemie.uni-wuerzburg.de

New Journal of Physics **15** (2013) 025006 (12pp)
Received 5 October 2012
Published 5 February 2013
Online at http://www.njp.org/
doi:10.1088/1367-2630/15/2/025006

Abstract. Using coherent two-dimensional (2D) electronic spectroscopy in fully noncollinear geometry, we observe the excitonic coupling of β,β'-linked bis[tetraphenylporphyrinato-zinc(II)] on an ultrafast timescale in the excited state. The results for two states in the Soret band originating from an excitonic splitting are explained by population transfer with approximately 100 fs from the energetically higher to the lower excitonic state. This interpretation is consistent with exemplary calculations of 2D spectra for a model four-level system with coupling.

[3] Present address: Bayer Pharma AG, Chemical Development, Friedrich-Ebert-Straße 217-333, D-42117 Wuppertal, Germany.
[4] Author to whom any correspondence should be addressed.

Contents

1. Introduction

The molecular class of tetrapyrroles has been a focus of research for a long time because they are relevant for many functions in nature. Famous examples are chlorophylls and bacteriochlorophylls, which are based on the fundamental structure of tetrapyrroles performing effective light and electron transfer [1, 2]. Furthermore, tetrapyrroles and their derivates have shown a variety of possible applications [3] including photodynamic therapy [4], chemical and biological sensors [5], molecular logic devices [6], optoelectronics [7] and their usage as synthetic light-harvesting and storage systems [8]. Many such applications require an understanding of the excited-state dynamics of porphyrins; for instance, light signal transmission in molecular photonic wires proceeds through excited-state energy transfer [9]. A powerful tool to investigate these dynamics is coherent two-dimensional (2D) electronic spectroscopy, as it separates signal contributions into excitation and detection frequencies [10], as shown, for example, in a conformation-dependent study for a porphyrin dimer in a fluorescence-based approach [11]. This separation allows for an intuitive understanding of population and energy transfer in complex photoactive systems [12–14].

In this study, we examine the excitonic dynamics of the directly β,β'-linked porphyrin dimer bis[tetraphenylporphyrinato-zinc(II)] [$(ZnTPP)_2$] in the Soret or B-band. As a result of the direct β,β'-linkage, the insertion of Zn, which rigidifies the molecular backbone, and steric hindrance because of the large phenyl substituents, $(ZnTPP)_2$ exhibits intrinsic axial chirality. Figure 1 shows the molecular structure (inset), steady-state absorption (black solid) of $(ZnTPP)_2$ [15, 16] dissolved in ethanol and the pump-pulse spectrum used for the 2D experiments (red dashed). The steady-state spectrum consists of the weaker absorption in the Q-band with maxima at 563 and 601 nm and the typical stronger absorption in the Soret band with its maxima at 428 and 443 nm resulting from excitonic Davydov splitting [17, 18]. A third state in the Soret band, which is higher in energy but weaker than the other two excitonic states, is located at 421 nm. As our pump pulses do not excite or detect this state, it will not be considered hereafter. We recently investigated the relaxation dynamics of $(ZnTPP)_2$ and its monomeric unit and compared them with different covalently linked porphyrins, using transient-absorption spectroscopy that covered the ultrafast dynamics from femtoseconds up to hundreds of microseconds and in a spectral range from 415 to 700 nm [19]. One of the results of that study was the variation of dynamical behavior across the Soret band. The absorption change of the energetically higher lying state decreased on a timescale of $\approx$100 fs; in contrast, the absorption change linked to the energetically lower lying state decreased on the microsecond timescale ($\approx$50 μs).

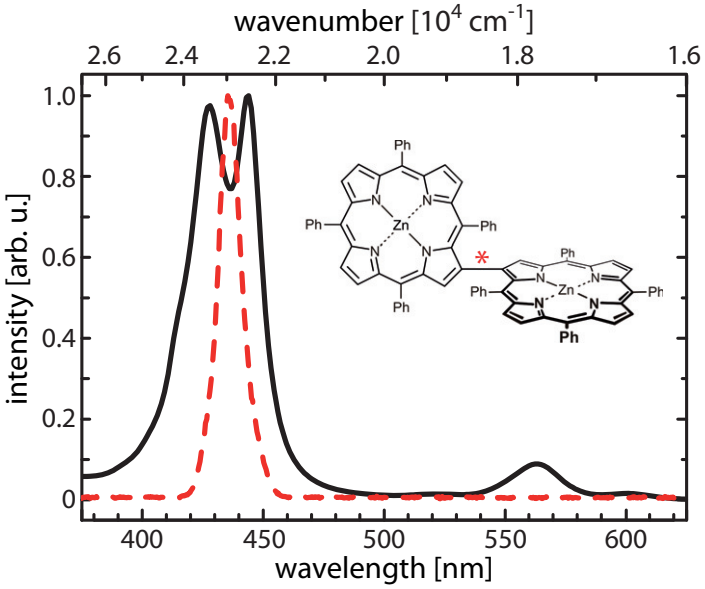

Figure 1. Linear absorption spectrum of $(ZnTPP)_2$ (black solid) and pump-pulse spectrum (red dashed) covering the excitonic states in the Soret band. The inset shows the molecular structure of one of the two enantiomers (with P-configuration; $*$ marks the configurationally stable, chiral biaryl axis).

Similar relaxation timescales were observed for other covalently linked porphyrin systems, e.g. by Hochstrasser [20] and Kim [21]. Hochstrasser and co-workers studied ethylene-bridged *meso*, *meso*′- and β,β'-linked dimers. They explained the photodynamics of the *meso*, *meso*′-linked dimer within a model comprising two conformers that differ in the dihedral angle between the porphyrin subunits. Kim and co-workers, who studied many porphyrin oligomers [22], adapted the two-conformer model by additionally including monomeric localized-excitation states and delocalized-excitonic states. The latter model was adapted for $(ZnTPP)_2$ in [19], and an alternative completely excitonic model was proposed to describe the relaxation dynamics, completely abstaining from monomeric localized-excitation states. Whereas the transient-absorption measurements gave a conclusive picture of the underlying processes, the states connected by coupling could only be inferred indirectly in the analysis. Therefore, in this work, we use 2D spectroscopy in order to directly visualize the predicted excitonic coupling in the Soret band.

2. Materials and methods

Spectroscopic experiments were performed by using a commercial steady-state absorption spectrometer (V 670, Jasco), a home-built femtosecond transient-absorption spectrometer setup and a 2D setup in fully noncollinear box geometry optimized for pulses in the ultraviolet regime [23].

In brief, laser pulses from a commercial Ti:sapphire regenerative-amplifier laser system (Spitfire Pro, Spectra-Physics, 800 nm, 1 kHz) were used to generate pulses centered at 870 nm in a commercial noncollinear optical parametric amplifier (TOPAS-White, Light Conversion). These pulses were afterwards frequency doubled in a 65 μm β-barium borate crystal leading

to pulses centered at 435 nm with 12 nm full-width at half-maximum and finally used for coherent 2D spectroscopy in an all-reflective, diffractive-optics-based, noncollinear four-wave mixing setup in phase-matched box geometry. The time resolution of approximately 50 fs was determined by transient grating measurements of pure ethanol at the sample position. Time delays were performed by a pairwise beam manipulation [23, 24] with a linear motorized delay stage (MFA CC, Newport) and piezo actuators (PX 200CAP, Piezosystem Jena). The obtained third-order signal was completely characterized by spectral interferometry with the help of a heterodyning local oscillator pulse [25] delayed by 1.8 ps and then detected with a charge-coupled device (CCD)-array spectrometer (Acton SpectraPro 2500i with PIXIS 2K, Princeton Instruments). The spectrum of the local oscillator was additionally recorded and then subtracted. Experimental artifacts caused by sample imperfections were removed by recording and subtracting two different scattering contributions [26]. For any population time T, the coherence time τ was scanned in 1.4 fs steps from -125 to $+125$ fs, moving excitation pulse 1 (2) in the second (first) half of the scanning period. Data analysis by Fourier transformation yielded the desired 2D traces, whose absolute phase was obtained by means of the projection-slice theorem and by comparison with separately recorded spectrally resolved pump–probe data [10, 26]. The absolute phase of the 2D traces for each population time was adjusted to the last measurement of each scan of T before averaging over several (2–5) T scans, thus minimizing contributions from a drift of the absolute phase over different scans. To avoid solvent effects and different signal contributions for short waiting times, the $T = 500$ fs 2D traces and pump–probe data were chosen for the phasing procedure.

The transient-absorption data were obtained by splitting the 435 nm pulses into two pulses via a 2 mm thick beamsplitter, resulting in a pump pulse with an energy of 4 nJ and a much weaker probe pulse, in mutual parallel polarization. Both pulses were focused onto the sample with spherical mirrors with the pump pulse traveling over an additional delay stage. The change in optical density was detected by measuring the spectrally dispersed probe with the CCD camera by a shot-to-shot technique and by blocking consecutive pump pulses. Comparability of the pump–probe and 2D measurements was achieved by avoiding dispersive elements with the sole exception being the thin beamsplitter. Data analysis was performed by obtaining lifetimes and spectral amplitudes with global parallel and sequential fitting routines [27] performed with the graphical interface GloTarAn [28] based on the statistical fitting package TIMP [29].

The measured porphyrin dimer $(ZnTPP)_2$ was synthesized according to the literature [15, 16], additionally purified by preparative gel permeation chromatography and analyzed by UV/Vis spectroscopy before and after optical experiments to exclude photodegradation. The molecule was dissolved in pure ethanol directly prior to time-resolved measurements with a concentration corresponding to an optical density of 0.3 at 443 nm in a 200 μm flow cell.

3. Results

Transient absorption data after direct excitation into and probing of the Soret band are shown in a contour plot in figure 2(a). Whereas the lower energetic peak shows only a small shift and nearly no decay with time, the higher energetic peak decreases and no spectral shift is visible. Two exemplary transients at the positions of the absorption peaks (compare figure 1) are shown in figure 2(b). The transient at 427 nm (blue) decreases after $\approx$100 fs, whereas the transient at 443 nm (red) shows almost no decay with time. The data shown here after excitation with 435 nm pulses are in accord with the 400 nm excitation used in the previous study [19].

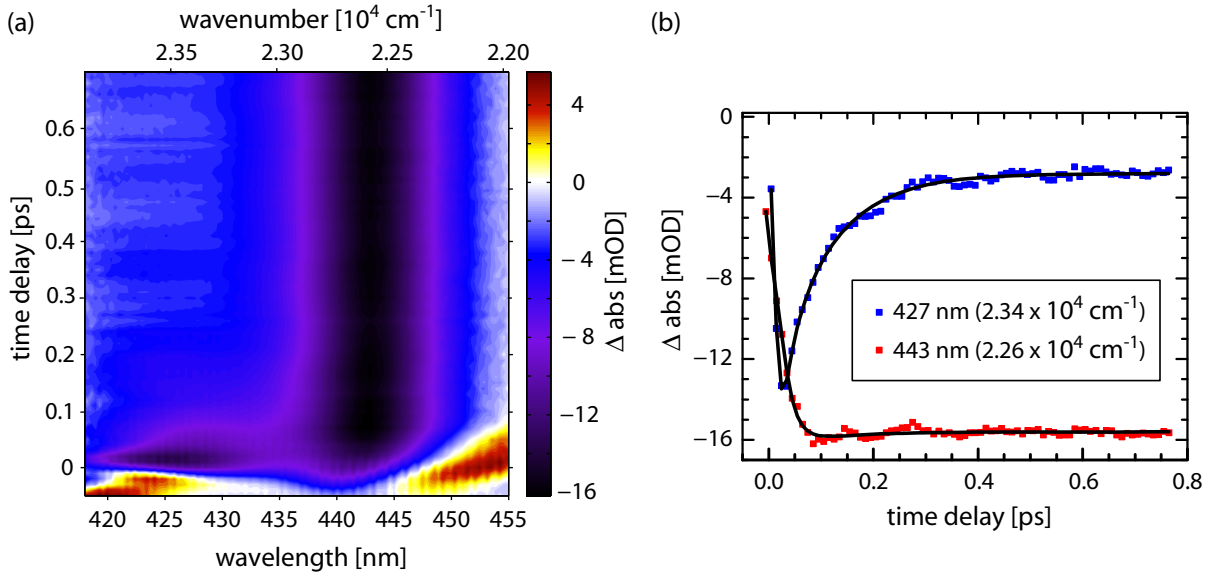

Figure 2. (a) Transient-absorption data of $(ZnTPP)_2$ covering the Soret band. (b) Transients reflecting the higher-energetic (blue) and lower-energetic (red) states together with the corresponding fits from global analysis (black).

The results from 2D spectroscopy are shown in figure 3 for several population times T in terms of absolute (Abs), absorptive real (Re) and refractive imaginary (Im) parts. Excitation corresponds to the horizontal $\bar{\nu}_\tau$ wavenumbers, and detection corresponds to the vertical $\bar{\nu}_t$ axis. As a consequence of the limited spectral width of the employed laser pulses, the dynamics of the two excitonic Soret states are visible as 2D line-shape modifications rather than clearly separated peaks. For the population time $T = 0$ fs, signal contributions of the solvent have to be taken into account. These signal contributions can be neglected for higher population times, as verified by transient grating and 2D measurements of the pure solvent. Furthermore, 'phase twist' contributions originating from the temporal overlap of the third pulse with the first two [30] may occur at $T = 0$ fs.

Considering the absolute and real parts, we observe a similar signal evolution over time. At the beginning ($T = 0$ fs) the signal containing both excitonic states is elongated along the diagonal of the spectra. In addition to the decrease of the signal intensity, the shape changes after a given time T from the diagonal orientation to a more circular and vertical shape. Along with the change in shape the signal contributions relax from higher to lower detection wavenumbers. The imaginary parts of the 2D spectra exhibit a change in sign. The connecting nodal plane changes from a diagonal to a vertical alignment with increasing T.

To obtain further insight into the dynamics, we show in figure 4(a) transient difference spectra for two pump-pulse frequencies corresponding to the two excitonic absorption maxima, labeled α and β. The difference spectra (DS_i), with $i = \alpha, \beta$ of the real parts with respect to the population time $T = 0$ fs, i.e. $I(T, \bar{\nu}_\tau^i, \bar{\nu}_t) - I(T = 0, \bar{\nu}_\tau^i, \bar{\nu}_t)$ are evaluated and the cuts along $\bar{\nu}_t$ for those $\bar{\nu}_\tau^i$ values corresponding to the linear absorption peaks ($\bar{\nu}_\tau^\alpha = -\bar{\nu}_\alpha = -2.26 \times 10^4\,\mathrm{cm}^{-1}$ and $\bar{\nu}_\tau^\beta = -\bar{\nu}_\beta = -2.34 \times 10^4\,\mathrm{cm}^{-1}$) are displayed. The combined GSB and SE signal of DS_α (red) decreases progressively at lower wavenumbers of $\bar{\nu}_t$. For DS_β (blue) the GSB and SE contributions change their magnitude with increasing population time; thus the

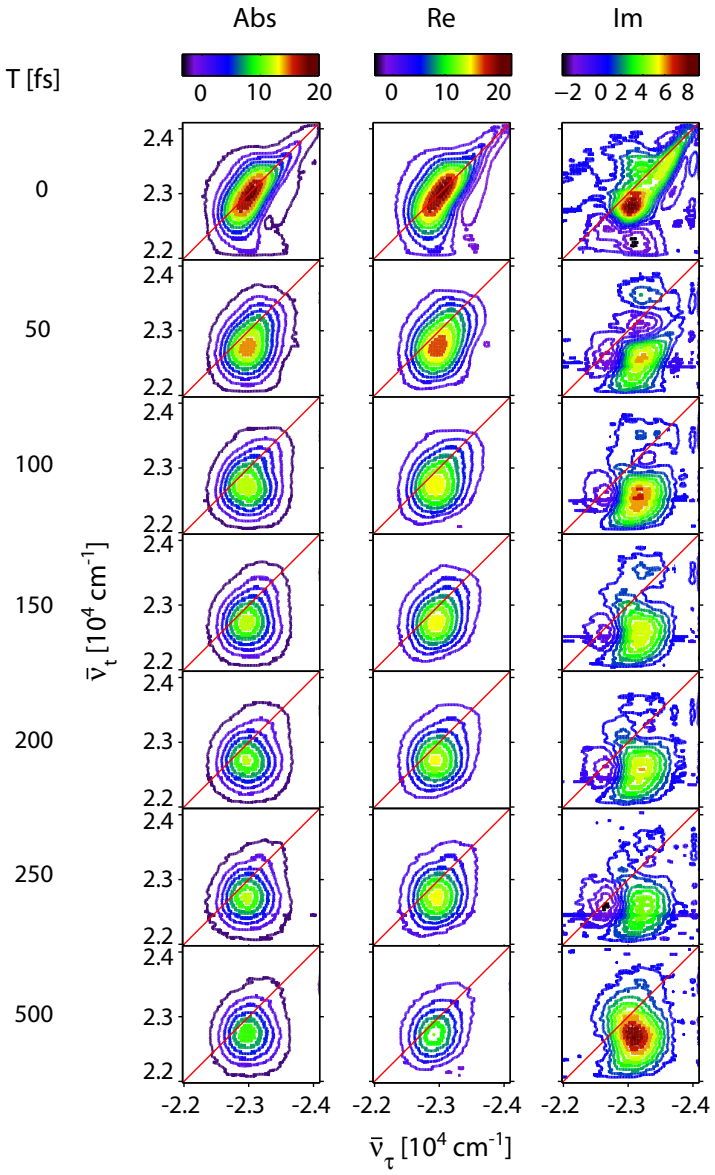

Figure 3. 2D data consisting of absolute (Abs), real valued (Re) and imaginary (Im) spectra for population times T in 50 fs steps and additionally for $T = 500$ fs. Contour lines from 5 to 95% of the maximum signal amplitude of the $T = 0$ fs data are drawn in steps of 10%. The color code is chosen to cover intensive positive (red) to negative (black) signal amplitudes; for example, the red and orange parts of the real 2D spectra indicate strong ground-state bleach (GSB) or stimulated emission (SE) signals.

difference spectrum shifts to lower wavenumbers. Additionally, a positive signal, indicative of increased absorption, at the lower energetic spectral region emerges after $T = 50$ fs and relaxes analogously.

In order to get a better impression of the different signal amplitude progressions in the 2D spectra, we chose four square regions of interest (ROI) with side lengths of 188 cm^{-1}

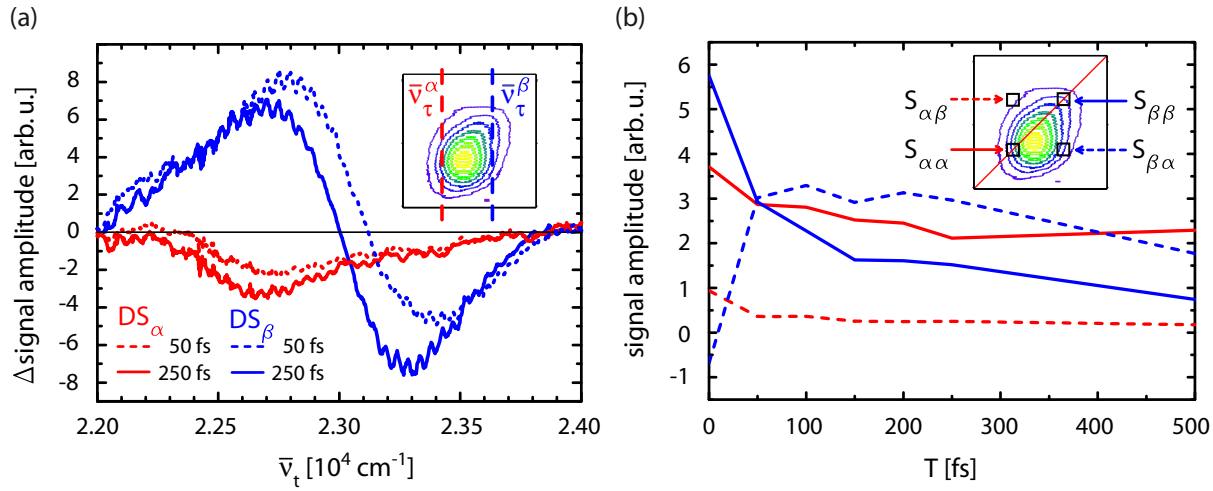

Figure 4. (a) Difference spectra with respect to $T = 0$ fs at $\bar{\nu}_\tau^\alpha = -2.26 \times 10^4\,\mathrm{cm}^{-1}$ (red) and $\bar{\nu}_\tau^\beta = -2.34 \times 10^4\,\mathrm{cm}^{-1}$ (blue) for $T = 50$ fs (dashed) and $T = 250$ fs (solid) as marked in the inset. (b) Development of diagonal and off-diagonal signal amplitudes for four ROI marked in the inset.

(corresponding to ≈3.5 nm) around the diagonal and off-diagonal wavenumbers corresponding to the linear absorption maxima. The signal evolution of these ROIs is shown in figure 4(b) as a function of population time for diagonal contributions at $S_{\alpha\alpha} = (-\bar{\nu}_\alpha, \bar{\nu}_\alpha)$, $S_{\beta\beta} = (-\bar{\nu}_\beta, \bar{\nu}_\beta)$ and off-diagonal signals at $S_{\alpha\beta} = (-\bar{\nu}_\alpha, \bar{\nu}_\beta)$ and $S_{\beta\alpha} = (-\bar{\nu}_\beta, \bar{\nu}_\alpha)$. Starting at $T = 0$ fs, only the diagonal signals (solid) show a significant positive amplitude. With increasing waiting time T both diagonal contributions decrease, reducing the amount of SE, although the signal amplitude of $S_{\beta\beta}$ decreases faster than $S_{\alpha\alpha}$. Considering the off-diagonal evolution (dashed), $S_{\alpha\beta}$ is positive at first, then shows a slight decay during the first femtoseconds and then remains close to zero. On the other hand, $S_{\beta\alpha}$ increases rapidly during the first 100 fs and subsequently decreases, remaining positive at the end.

4. Discussion

In our experiments, we excite and detect the dynamics of excitonic states in the Soret band of $(ZnTPP)_2$. Looking at the transient-absorption data in figure 2, a slight Stokes shift in the lower-energetic band can be seen since the main absorption wavelength shifts from 441 nm ($2.268 \times 10^4\,\mathrm{cm}^{-1} > \bar{\nu}_\alpha$) to 443 nm ($2.257 \times 10^4\,\mathrm{cm}^{-1} \approx \bar{\nu}_\alpha$) within 250 fs. This time also corresponds well to the lifetime of the Soret band in porphyrins as previously shown by Hochstrasser and co-workers [20] and confirmed for $(ZnTPP)_2$ by us [19]. This shift is evident considering the behavior on both sides of the absorption band and how the spectral position changes with time. The observed shift corresponds to a wavenumber difference of roughly $100\,\mathrm{cm}^{-1}$. By contrast, no such feature can be found for the higher-energetic Soret band corresponding to $\bar{\nu}_\beta$. Looking at the 2D spectra in figure 3, this relaxation has to be considered in the interpretation of the data. However, it is presumably not the main reason for the change in signal amplitude shown in the ROIs corresponding to the absorption at $\bar{\nu}_\beta$ ($S_{\beta\beta}$, $S_{\beta\alpha}$, figure 4(b)) since $\bar{\nu}_\beta$ is well above the

observed maximum frequency shift; thus the changes at $\bar{\nu}_\beta$ indicate the participation of other processes.

To discuss our results further, we chose a simple four-level model shown in figure 5(a) consisting of the ground state $|g\rangle$, the exciton states $|\alpha\rangle$ and $|\beta\rangle$ corresponding to the splitting in the Soret band and the two-exciton state $|f\rangle$ which implies that $|\alpha\rangle$ and $|\beta\rangle$ are both excited [18] (for a more elaborate modeling of similar systems, see, e.g., [31, 32]). The depicted transition wavenumbers $\bar{\nu}_{xy}$ correspond to the energy difference between the states $|x\rangle$ and $|y\rangle$ referring to the absorption maxima in the linear spectrum.

A look at the transient absorption data in figure 2 reveals a signal decay in $|\beta\rangle$ on a timescale of 100 fs. The product state is not unambiguously identified but $|g\rangle$ can be excluded, since then $|\alpha\rangle$ would need to show a similar signal decay: a populated ground state would enable reexcitation into both $|\alpha\rangle$ and $|\beta\rangle$ [19]. A reasonable assumption within the model is a population transfer from $|\beta\rangle$ to $|\alpha\rangle$, which would lead to an increased excited-state absorption into the two-exciton state $|f\rangle$. Looking at the behavior in $|\alpha\rangle$, only a small Stokes shift or a vanishing SE signal on a femtosecond timescale is directly observable, but the amount of bleaching stays roughly the same over the entire delay time. This evidences that the ground state is not repopulated during the experiment.

By considering the development of the signal amplitude and the simultaneous change in shape to lower energies in the real-valued 2D spectra in figure 3, the relaxation process is also evident. Besides the simple overall relaxation observable in all spectra into the lower Q-band [19] (as also known for similar systems [20, 21]) which manifests itself only indirectly in this study, since then no SE from S_2 is possible anymore, the signal amplitude for high excitation $\bar{\nu}_\tau$ and low detection $\bar{\nu}_t$ wavenumbers changes with time. This indicates a relaxation by solvent effects such as a Stokes shift or by a population transfer from $|\beta\rangle$ to $|\alpha\rangle$, as the change mainly appears as an off-diagonal signal between the corresponding excitonic states.

The changes in the signal amplitude are more precisely seen in the difference spectra (compare figure 4(a)) relative to $T = 0$ fs. For DS_α a weaker decrease of signal amplitude compared to DS_β can be observed, which confirms the different dynamics already seen in transient absorption and the higher stability of $|\alpha\rangle$. Comparing the difference spectra for $T = 50$ and 250 fs, a progressive decrease to lower wavenumbers of the combined SE and GSB signal can be observed. At $T = 0$ the signal consists of GSB and SE contributions. After a given population time ($T = 50$ fs) the signal shifts to lower wavenumbers as the SE contribution is influenced by a Stokes shift. As the lifetime in the Soret band is ≈ 150 fs [20] the Stokes-shifted SE vanishes for $T \gg 150$ fs while the GSB is still maintained, leading to the observed stronger signal decrease at lower wavenumbers. The most important additional feature is an increasing signal amplitude for DS_β at wavenumbers corresponding to the lower energetic state $|\alpha\rangle$, which is a consequence of a coupling between $|\beta\rangle$ and $|\alpha\rangle$. This signal is indicative of relaxation from $|\beta\rangle$ into $|\alpha\rangle$ since molecules excited into $|\beta\rangle$ now show absorption at frequencies corresponding to the state $|\alpha\rangle$ while at the same time the SE signal for $|\beta\rangle$ decreases.

The same dynamics can be seen in the development of the signal amplitudes at the chosen ROIs in figure 4(b). The decreasing amplitudes $S_{\alpha\alpha}$ and $S_{\beta\beta}$, which monitor the number of molecules that stay in their excited state, mirror the observation of the transient absorption study and show an overall decrease again much faster for $S_{\beta\beta}$ than for $S_{\alpha\alpha}$. After a given population time the dynamics are dominated by population relaxation processes from $|\beta\rangle$ to $|\alpha\rangle$. As this relaxation gives rise to contributions to the excited-state absorption for $S_{\beta\beta}$ and to the SE for

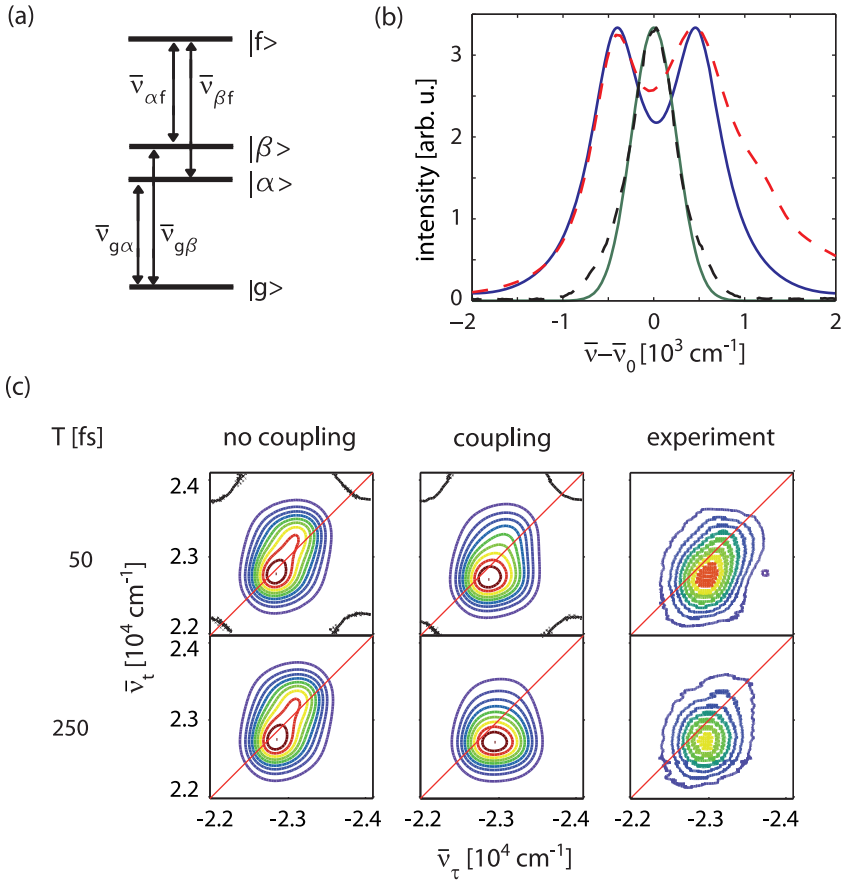

Figure 5. (a) Four-level model consisting of the ground state $|g\rangle$, excitonic states $|\alpha\rangle$, $|\beta\rangle$ and biexcitonic state $|f\rangle$. (b) Fit with two Lorentzians (blue) to the measured linear absorption spectrum (dashed red) and Gaussian fit (green) to the experimental pump pulse spectrum (dashed black). (c) Calculated real-valued 2D spectra in an excitonic system without coupling (left), with coupling (middle) and corresponding experimental data (right) for $T = 50$ fs (top) and $T = 250$ fs (bottom).

$S_{\beta\alpha}$, it explains the time evolution of the related signal amplitudes, an increase for $S_{\beta\alpha}$ and a decrease for $S_{\beta\beta}$ as long as this transfer takes place.

Furthermore, in order to separate this contribution from relaxation processes such as a Stokes shift, we calculated the real-valued 2D spectra in the four-level system (figure 5(a)). In the simulated data, the corresponding excitonic states were fitted by Lorentzian functions to the linear absorption spectrum and the excitation and detection pulses were treated by Gaussian functions (figure 5(b)). The calculations were performed with and without the inclusion of a coupling between the excitonic states to compare these with the experimental results (figure 5(c)), whereas no additional environmental and inhomogeneous broadening effects were considered. Moreover, to keep the model as simple as possible we did not include a relaxation to S_1 states (Q-bands) or triplet states as will occur in porphyrins. The coupling was taken into account by an exponential population transfer from $|\beta\rangle$ to $|\alpha\rangle$ with a time constant of 114 fs [19]. Considering the simulated spectra without coupling, the signal starts

in a diagonal orientation and changes slightly to lower detection frequencies with evolving time. This qualitative behavior is not a good match for the experimental observations. On the other hand, the coupled calculation shows a shift of intensity for high excitation wavenumbers going from higher to lower detection wavenumbers with time, i.e. a growth of contributions below the diagonal. In addition, the diagonal orientation for small T becomes horizontally symmetric with time. Compared with the experiment the development of the spectral shape resembles the calculated coupled 2D spectra qualitatively, especially a shift of the center of gravity to regions below the diagonal is evident. Hence, regarding both the measurements and the simulated model spectra, we consider population transfer within the excited Soret band to be a reasonable explanation for the observed effects.

5. Conclusions

In this study, we have presented the ultrafast excitonic dynamics in the Soret band of the directly β,β'-linked porphyrin dimer $(ZnTPP)_2$, analyzed by transient absorption and coherent 2D spectroscopy. In the transient-absorption experiments the relaxation dynamics of the excitonic states clearly differ, but only an indirect assignment of the involved states is possible. We investigate these relaxation dynamics in more detail and assign them using coherent 2D spectroscopy. Data analysis shows that these dynamics cannot result from a Stokes shift alone, but off-diagonal contributions in the experimental and qualitatively modeled 2D spectra provide an explanation: population transfer occurs between the corresponding excitonic states as a result of electronic coupling. This population transfer is in accord with previous studies of different covalently linked porphyrins [20, 21] and was directly observed here, substantiating the interpretation in the framework of excitonic coupling [18]. $(ZnTPP)_2$ may serve as an exemplary system exhibiting excitonic dynamics that are directly reflected in off-diagonal contributions in 2D spectra of electronically coupled chromophores [31, 32]. Moreover, this study contributes to a deeper understanding of the processes happening in the strongly absorbing yet very short-lived Soret bands of porphyrins, which may prove beneficial for some of the versatile porphyrin applications ranging from catalysis to biomimicry of electron transfer [16].

Acknowledgments

We acknowledge funding from the German Research Foundation (DFG) through the Research Unit ‘Light-Induced Dynamics in Molecular Aggregates’ (FOR 1809). PN also acknowledges the DFG for support within the Emmy-Noether program. DCGG gratefully acknowledges the Studienstiftung des deutschen Volkes eV for financial support. We thank Andreas Steinbacher for his help with the analysis software. This publication was funded by the DFG and the University of Wuerzburg under the funding program Open Access Publishing.

References

[1] Hall D O and Rao K K 1999 *Photosynthesis* vol 6 (Cambridge: Cambridge University Press)
[2] Kadish K M, Guilard R and Smith K M 2010 *Handbook of Porphyrin Science: With Applications to Chemistry, Physics, Materials Science, Engineering, Biology and Medicine* vol 1 (Singapore: World Scientific)
[3] Tripathy U and Steer R P 2007 The photophysics of metalloporphyrins excited in their Soret and higher energy UV absorption bands *J. Porphyr. Phthalocya.* **11** 228–43

[4] Sternberg E D, Dolphin D and Brückner C 1998 Porphyrin-based photosensitizers for use in photodynamic therapy *Tetrahedron* **54** 4151–202
[5] Mirkin C A and Ratner M A 1992 Molecular electronics *Annu. Rev. Phys. Chem.* **43** 719–54
[6] Remacle F, Speiser S and Levine R D 2001 Intermolecular and intramolecular logic gates *J. Phys. Chem.* B **105** 5589–91
[7] Lammi R K, Ambroise A, Balasubramanian T, Wagner R W, Bocian D F, Holten D and Lindsey J S 2000 Structural control of photoinduced energy transfer between adjacent and distant sites in multiporphyrin arrays *J. Am. Chem. Soc.* **122** 7579–91
[8] Patten P G V, Shreve A P, Lindsey J S and Donohoe R J 1998 Energy-transfer modeling for the rational design of multiporphyrin light-harvesting arrays *J. Phys. Chem.* B **102** 4209–16
[9] Yoon M, Jeong D H, Cho S, Kim D, Rhee H and Joo T 2003 Ultrafast transient dynamics of Zn(II) porphyrins: observation of vibrational coherence by controlling chirp of femtosecond pulses *J. Chem. Phys.* **118** 164
[10] Jonas D M 2003 Two-dimensional femtosecond spectroscopy *Annu. Rev. Phys. Chem.* **54** 425–63
[11] Lott G A, Perdomo-Ortiz A, Utterback J K, Widom J R, Aspuru-Guzik A and Marcus A H 2011 Conformation of self-assembled porphyrin dimers in liposome vesicles by phase-modulation 2D fluorescence spectroscopy *Proc. Natl Acad. Sci. USA* **108** 16521–6
[12] Brixner T, Stenger J, Vaswani H M, Cho M, Blankenship R E and Fleming G R 2005 Two-dimensional spectroscopy of electronic couplings in photosynthesis *Nature* **434** 625–8
[13] Kullmann M, Ruetzel S, Buback J, Nuernberger P and Brixner T 2011 Reaction dynamics of a molecular switch unveiled by coherent two-dimensional electronic spectroscopy *J. Am. Chem. Soc.* **133** 13074–80
[14] Bixner O *et al* 2012 Ultrafast photo-induced charge transfer unveiled by two-dimensional electronic spectroscopy *J. Chem. Phys.* **136** 204503
[15] Bringmann G, Rüdenauer S, Götz D C G, Gulder T A M and Reichert M 2006 Axially chiral directly β, β'-linked bisporphyrins: synthesis and stereostructure *Org. Lett.* **8** 4743–6
[16] Bringmann G, Götz D C G, Gulder T A M, Gehrke T H, Bruhn T, Kupfer T, Radacki K, Braunschweig H, Heckmann A and Lambert C 2008 Axially chiral β, β'-bisporphyrins: synthesis and configurational stability tuned by the central metals *J. Am. Chem. Soc.* **130** 17812–25
[17] Kasha M, Rawls H R and El-Bayoumi M A 1965 The exciton model in molecular spectroscopy *Pure Appl. Chem.* **11** 371–92
[18] van Amerongen H, Valkunas L and van Grondelle R 2000 *Photosynthetic Excitons* (Singapore: World Scientific)
[19] Kullmann M, Hipke A, Nuernberger P, Bruhn T, Götz D C G, Sekita M, Guldi D M, Bringmann G and Brixner T 2012 Ultrafast exciton dynamics after Soret- or Q-band excitation of a directly β, β'-linked bisporphyrin *Phys. Chem. Chem. Phys.* **14** 8038–50
[20] Kumble R, Palese S, Lin V S, Therien M J and Hochstrasser R M 1998 Ultrafast dynamics of highly conjugated porphyrin arrays *J. Am. Chem. Soc.* **120** 11489–98
[21] Cho H S, Song N W, Kim Y H, Jeoung S C, Hahn S, Kim D, Kim S K, Yoshida N and Osuka A 2000 Ultrafast energy relaxation dynamics of directly linked porphyrin arrays *J. Phys. Chem.* A **104** 3287–98
[22] Kim D and Osuka A 2003 Photophysical properties of directly linked linear porphyrin arrays *J. Phys. Chem.* A **104** 8791–816
[23] Selig U, Schleussner C, Foerster M, Langhojer F, Nuernberger P and Brixner T 2010 Coherent two-dimensional ultraviolet spectroscopy in fully noncollinear geometry *Opt. Lett.* **35** 4178–80
[24] Cowan M L, Ogilvie J P and Miller R J D 2004 Two-dimensional spectroscopy using diffractive optics based phased-locked photon echoes *Chem. Phys. Lett.* **386** 184–9
[25] Lepetit L and Joffre M 1996 Two-dimensional nonlinear optics using Fourier-transform spectral interferometry *Opt. Lett.* **21** 564–6
[26] Brixner T, Mančal T, Stiopkin I V and Fleming G R 2004 Phase-stabilized two-dimensional electronic spectroscopy *J. Chem. Phys.* **121** 4221–36
[27] van Stokkum I H M, Larsen D S and van Grondelle R 2004 Global and target analysis of time-resolved spectra *Biochim. Biophys. Acta Bioenerg.* **1657** 82–104

[28] Snellenburg J J, Laptenok S P, Seger R, Mullen K M and van Stokkum I H M 2012 Glotaran: a Java-based graphical user interface for the R-package TIMP *J. Stat. Softw.* **49** 1–22

[29] Mullen K M and van Stokkum I H M 2007 TIMP: an R package for modeling multi-way spectroscopic measurements *J. Stat. Softw.* **18** 1–46

[30] Gallagher Faeder S M and Jonas D M 1999 Two-dimensional electronic correlation and relaxation spectra: theory and model calculations *J. Phys. Chem.* A **103** 10489–505

[31] Kjellberg P, Brüggemann B and Pullerits T 2006 Two-dimensional electronic spectroscopy of an excitonically coupled dimer *Phys. Rev.* B **74** 024303

[32] Szöcs V, Pálszegi T, Lukeš V, Sperling J, Milota F, Jakubetz W and Kauffmann H F 2006 Two-dimensional electronic spectra of symmetric dimers: intermolecular coupling and conformational states *J. Chem. Phys.* **124** 124511